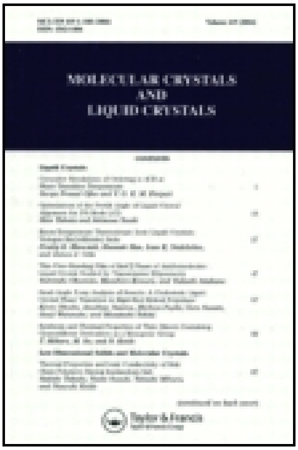

Molecular Crystals and Liquid Crystals
Publication details, including instructions for authors and subscription information:
http://www.tandfonline.com/loi/gmcl20

Unentangled Rheological Behavior of a Nematic Azobenzene Polymethacrylate

Laura Andreozzi [a] , Ciro Autiero [a] , Massimo Faetti [a] , Marco Giordano [a] , Fabio Zulli [a] & Giancarlo Galli [b]
[a] Dipartimento di Fisica, Università di Pisa, and polyLab INFM, Pisa, Italy
[b] Dipartimento di Chimica e Chimica Industriale, Università di Pisa, and INSTM, Pisa, Italy

Version of record first published: 18 Mar 2009

To cite this article: Laura Andreozzi, Ciro Autiero, Massimo Faetti, Marco Giordano, Fabio Zulli & Giancarlo Galli (2009): Unentangled Rheological Behavior of a Nematic Azobenzene Polymethacrylate, Molecular Crystals and Liquid Crystals, 500:1, 63-72

To link to this article: http://dx.doi.org/10.1080/15421400802713694

Mol. Cryst. Liq. Cryst., Vol. 500, pp. 63–72, 2009
Copyright © Taylor & Francis Group, LLC
ISSN: 1542-1406 print/1563-5287 online
DOI: 10.1080/15421400802713694

Unentangled Rheological Behavior of a Nematic Azobenzene Polymethacrylate

Laura Andreozzi[1], Ciro Autiero[1], Massimo Faetti[1], Marco Giordano[1], Fabio Zulli[1], and Giancarlo Galli[2]
[1]Dipartimento di Fisica, Università di Pisa, and polyLab INFM,
Pisa, Italy
[2]Dipartimento di Chimica e Chimica Industriale, Università di Pisa,
and INSTM, Pisa, Italy

The rheological behavior of a nematic polymethacrylate containing an azobenzene side group was investigated. The time-temperature superposition principle was found to hold over a large temperature range, as no discontinuities were detected at the isotropic-nematic transition temperature, despite the relatively high molar mass of the polymer. A direct proof of the unentangled behavior of the polymer is provided, which stems from a dynamic model able to predict the relaxation mechanisms by simply knowing the molar mass distribution of the polymer sample.

Keywords: azobenzene; entanglement; liquid crystal polymer; nematic; rheology

INTRODUCTION

Polymers carrying azobenzene side groups are the focus of active research since a number of years; for late examples, see e.g. [1–3]. Especially, polymers in which the azobenzene acts as both a mesogenic and a photoresponsive group hold promise in a diversity of applications in optics, non-linear optics and optoelectronics [4].

We recently accomplished optical writing at both micrometer and nanometer length scales in the nematic polymethacrylate PMA4

The authors thank the Regione Toscana, POR Ob.3 D4, for partial financial support of the work.

Address correspondence to Laura Andreozzi, Dipartimento di Fisica, Università di Pisa, and polyLab INFM, largo Pontecorvo, 3, 56127 Pisa, Italy. E-mail: laura.andreozzi@df.unipi.it

system (homopolymer and copolymers) [5–7] (Fig. 1). Bit stability, homogeneity at molecular level, and working temperature range were found to be crucial materials parameters to achieve an effective, high-resolution and long-term data storage. Thus, studies that cover different time and length scales must be employed in order to fully characterize these polymers and the mechanisms driving their relaxation. In this work, we carried out a rheological investigation on a PMA4 homopolymer of relatively high molar mass and show that the polymer dynamics can be well predicted by models referring to unentangled chains.

MATERIALS AND EXPERIMENTAL

The PMA4 homopolymer ($x = 1.0$ in Fig. 1), denoted here as S5, was prepared by free-radical polymerization according to literature [8].

Its molar mass distribution was determined by size exclusion chromatography (SEC) of chloroform solutions with a 590 Waters chromatograph equipped with two Shodex KF804 columns and both RI R401 and UV LC75 detectors. Polystyrene standard samples (M_n in the range $1 \times 10^3 - 5 \times 10^5$ g/mol) were used for the calibration. Figure 2 shows the experimental SEC curve of the sample. The values of the number-average M_n and weight-average M_w molar masses and the polydispersity index M_w/M_n are shown in Table 1.

Differential scanning calorimetry (DSC) measurements were performed with a Perkin-Elmer DSC7 calorimeter (10 K/min heating rate) calibrated with indium and zinc standards. In addition to the glass transition temperature T_g and the nematic-isotropic temperature T_{ni}, the DSC traces also evidenced a change in heat capacity associated with a conformational transition at the onset temperature T_c of 337 K [9] (Fig. 3). Previous LODESR spectroscopy studies suggested that this transition is driven by the increasing nematic order as the temperature was lowered [7].

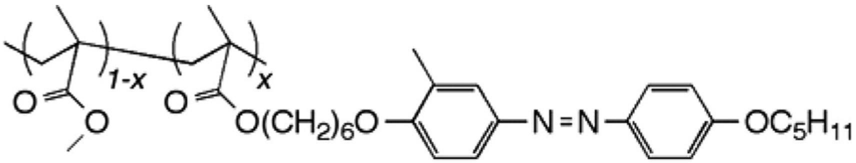

FIGURE 1 Chemical structure of PMA4 polymers: homopolymers are represented by $x = 1$, random copolymers by $0 < x < 1$.

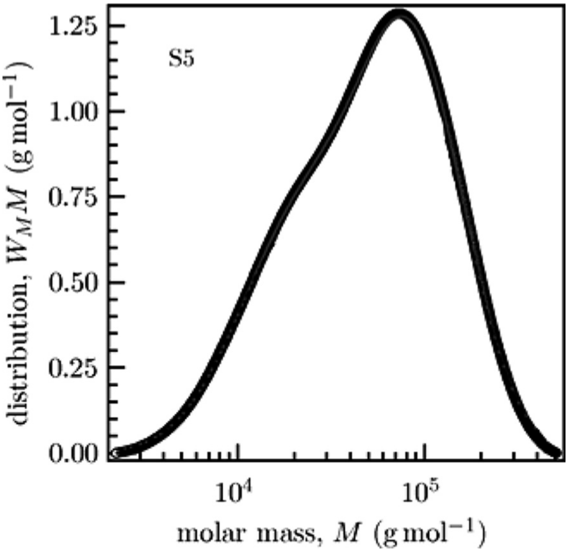

FIGURE 2 SEC molar mass distribution of the PMA4 homopolymer S5.

A Haake RheoStress RS150H rheometer in the plane-plate geometry (20 mm diameter) was employed for the linear viscoelastic characterization of the PMA4 sample. Measurements were carried out in the temperature range 313–413 K under highly pure nitrogen flow. The gap in the sensor geometry was automatically varied in the temperature range between 0.40 mm and 0.60 mm in order to account for thermal dilatation of the system. A significantly larger gap was chosen than the chain length to ensure gap-independent measurements. The sample temperature was stable within 0.1 K. To make sure that all measurements were carried out in the linear regime, preliminary tests on viscoelastic linearity of the materials were conducted.

TABLE 1 Average Molar Masses and Transition Temperatures for the PMA4 Homopolymer S5

M_n (g/mol)	M_w (g/mol)	M_w/M_n	T_g (K)	T_c (K)	T_{ni} (K)
29900	72600	2.43	305	337	357

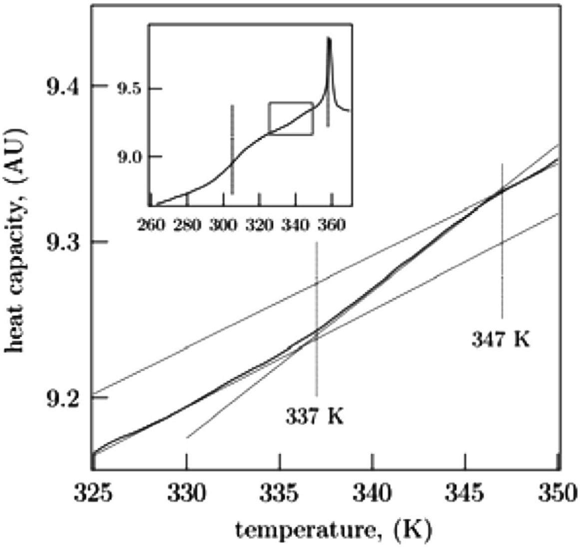

FIGURE 3 DSC scan of the PMA4 homopolymer S5. In the inset, the whole thermogram is shown. The conformational transition is highlighted.

RESULTS AND DISCUSSION

In Figure 4, experimental values of the zero-shear viscosity obtained by oscillatory measurements and direct creep measurements are shown as a function of $1000/T$. No discontinuities of the viscosity were observed at the T_c or T_{ni} for the homopolymer. This allowed to fit the viscosity data with a Vogel-Fulcher law (VF) [10]:

$$\eta(T) = \eta_\infty \exp\left(\frac{T_b}{T - T_0}\right) \tag{1}$$

The values of the factor η_∞, the pseudo-activation temperature T_b, and the Vogel temperature T_0 are reported in Table 2.

On the other hand, in the whole investigated temperature range, the time-temperature superposition (TTS) principle was found to be applicable to the storage G' and loss G'' moduli of the homopolymer (Fig. 5) in the nematic and the isotropic phases, and also across the conformational transition temperature. This confirms that the TTS principle holds for this side-group polymer, indicating that the rheological properties are dominated by the polymer backbone dynamics. In fact, previous results on similar liquid crystalline polymers [11,12] only showed a failure of TTS for samples with very high molar masses

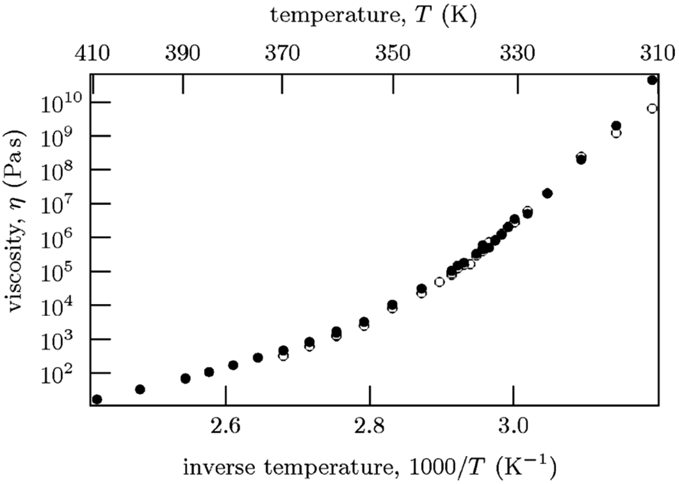

FIGURE 4 Dynamic (open circles) and creep (bullets) viscosity as a function of $1000/T$ for PMA4 homopolymer S5.

[11], at least one order of magnitude larger than that of the present PMA4 sample. Failures of TTS are instead expected for main-chain liquid-crystalline polymers [11].

Mathematical shift of the experimental isothermal frequency sweeps of the complex modulus G^* [13,14] led to the calculation of master curves (Fig. 6) and horizontal $a_{T_r}(T)$ and vertical shift factors at the reference temperature $T_r = 338\,\mathrm{K}$. The temperature dependence of the horizontal shift factor $a_{T_r}(T)$ was well described by the Williams-Landel-Ferry (WLF) law [10]:

$$\log a_{T_r}(T) = \frac{-c_1(T - T_r)}{T - T_r + c_2}. \tag{2}$$

The quantities c_1 and c_2 are the so-called WLF parameters, and T_r is the reference temperature. The values of the WLF parameters c_1 and c_2 are shown in Table 3.

TABLE 2 VF Parameters of the PMA4 Homopolymer S5

η_∞ (Pa s)	T_b (K)	T_0 (K)
$(3.7 \pm 0.1) \times 10^{-3}$	1100 ± 30	278 ± 3

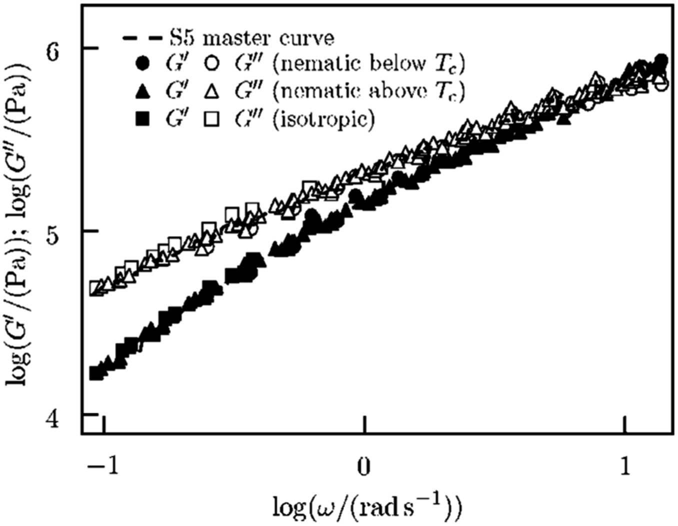

FIGURE 5 Master curve for the PMA4 homopolymer S5 in different phases. Superimposed complex modulus is shown at various reference temperatures in different phases: isotropic (bullets), nematic above T_c, (triangles), nematic below T_c (circles).

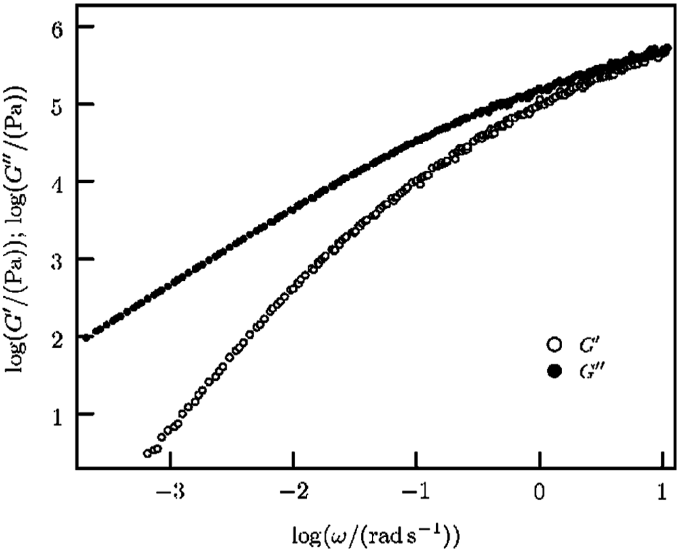

FIGURE 6 Experimental master curves of storage and loss moduli of the PMA4 homopolymer S5 at the reference temperature $T_r = 338\,\mathrm{K}$.

TABLE 3 WLF Parameters of the PMA4 Homopolymer S5. Parameters Extrapolated at T_g Are Also Given

c_1	c_2 (K)	T_r (K)	$c_1c_2 \ln 10$ (K)	$T_r - c_2$ (K)	c_1^g	c_2^g (K)
8.0 ± 0.1	60 ± 1	338.0 ± 0.1	1100 ± 40	278 ± 1	18 ± 2	27 ± 2

According to TTS and Doolittle equation [13, and references therein], the relationships

$$\begin{aligned} T_b &= c_1c_2 \ln 10 \\ T_0 &= T_r - c_2 \end{aligned} \tag{3}$$

can be found between VF and WLF parameters if the values of vertical shift parameters are about one. In this event, the same temperature dependence can be found for viscosity and horizontal shift parameters. This behavior was confirmed for the present PMA4 homopolymer.

It is apparent that c_1 and c_2 are T_r-dependent parameters, while c_1c_2 and $T_r - c_2$ are T_r-independent quantities. Fit parameters of the homopolymer confirmed these relations within the experimental error (Table 3). In addition to this, being c_1c_2 and $T_r - c_2$ constants independent of T_r, it is also possible to remove any further chain-ends dependence in c_1 and c_2 by extrapolating the WLF parameters at T_g: c_1^g and c_2^g. These values are usually found to be similar in homologous samples [13]. This behavior is also shown by PMA4 samples [15], providing a further confirmation that rheological properties are dominated by polymer backbone [11].

Let us now examine the master curve of the PMA4 homopolymer shown in Figure 6. The typical liquid behavior is observed in the low frequency side, as expected of linear homopolymers. Quite unexpectedly, a rubbery plateau, characteristic of entangled chain dynamics of polymers with molar masses higher than the entanglement molar mass ($M > M_e$) [16,17], is missing. In fact, such a plateau appears in various acrylic polymers roughly at a critical molar mass $M_c' \approx 3M_e$ in the range 24000–40000 g/mol [16]. The absence of entanglement was also previously inferred from the dynamic modulus of several analogous azobenzene polymethacrylates [12], even possessing molar masses expected to be above M_c'. Possibly, the nematic order dilates the confining tube [12], on which dimension the M_e value depends [16], and shifts entanglement to higher molar masses.

Confirmation of the unentangled behavior of the PMA4 homopolymer was gained by calculation of the master curve according to the Rouse model. Among the working hypotheses of Rouse model, in fact, one has to include that the polymer backbone is not hampered by constraints introduced by the neighboring chains [17]. Spacer segments connecting the azobenzene side groups to the main chain prevent the nematic potential to affect directly the motion of the backbone. Conversely, topological constraints, such as entanglement, make the Rouse model unable to predict the polymer dynamics. According to the Rouse model, the complex modulus of a monodisperse melt of density ρ and molar mass M obtained as a summation over the p-th dynamic modes is:

$$G^*_{\text{mono}}(\omega, M) = \frac{\rho RT}{M} \sum_{p>0} \left(\frac{\omega^2 \tau_R^2}{4p^4 + \omega^2 \tau_R^2} + i \frac{2p^2 \omega \tau_R}{4p^4 + \omega^2 \tau_R^2} \right), \tag{4}$$

$$\tau_R = \frac{\zeta_0 b^2 N_A}{3\pi^2 RT} N^2 = K_R \frac{M^2}{M_0^2}. \tag{5}$$

The Rouse relaxation time τ_R depends on the gas constant R, the Avogadro number N_A, the temperature T, the number N of beads and rest length b of springs in the beads-and-springs model employed to develop the Rouse theory [17]. Also, the Rouse relaxation time can be written as the product of the square of the ratio of the molar mass of the chain M to the molar mass of a repeating unit M_0 (where $M/M_0 = N$) and a mass-independent factor K_R. Besides T, the only temperature-dependent quantity in Eq. (5) is the monomeric friction coefficient ζ_0, whose temperature dependence is expected to be the same as for viscosity [13].

The total complex shear modulus G^* is given by the contribution of the overall monodisperse components $G^*_{\text{mono}}(\omega, M)$ of the molar mass distribution $w(M) = \mathrm{d}W(M)/\mathrm{d}\log M$, where $W(M)$ is the weight fraction of chains with molar mass lower than M:

$$G(\omega) = \int w(M) G^*_{\text{mono}}(\omega, M) \, \mathrm{d}\log M. \tag{6}$$

To compute master curves, a numerical algorithm was written. The only free parameter is the mass-independent factor K_R of the Rouse time (Eq. (5)). The experimental master curves agreed very well with the calculated storage and loss moduli (Fig. 7). The factor K_R was found to be $(3.10 \pm 0.05) \times 10^{-4}$ s. This proves that the Rouse model is able to describe the mechanical response of the PMA4 homopolymer, providing further evidence that the melt is unentangled, and indicating that ordinary models of polymer dynamics also hold for this side-chain liquid crystalline polymer.

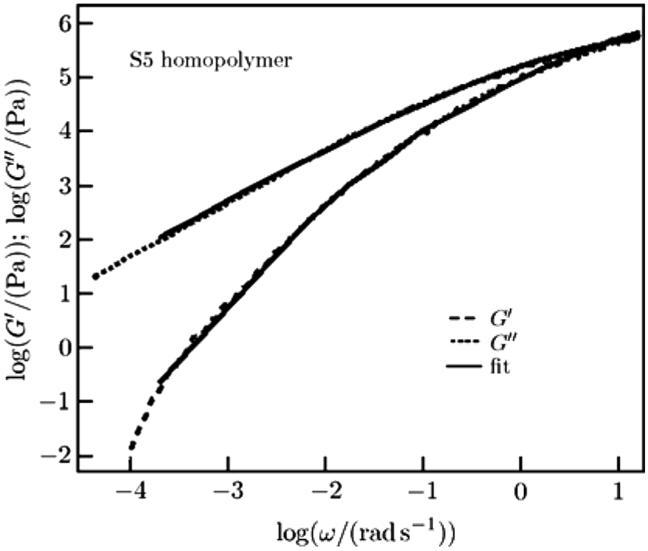

FIGURE 7 Master curve calculation of the PMA4 homopolymer S5 according to the Rouse model (solid line). For comparison, the experimental storage and loss moduli of Figure 6 are also reported (dashed and dotted lines, respectively). χ_r^2 was found to be 0.3.

CONCLUSIONS

The linear viscoelastic behavior of the PMA4 homopolymer with relatively high molar mass shows that the TTS principle holds even across the transition temperatures. Moreover, a substantial equivalence of VF and WLF laws is also observed. Fitting of G^* master curve with the theoretical modulus calculated by the Rouse model provides direct confirmation of an unentangled behavior, by contrast to expectations of polymer chain entanglement. Such calculation also allows one to easily predict the dynamic response of any unentangled PMA4 homologous homopolymer, by merely knowing the molar mass distribution of the polymer sample.

REFERENCES

[1] Lanzi, M., Paganin, L., & Cesari, G. (2008). *Macromol. Chem. Phys.*, *209*, 375.
[2] Bang, C.-U., Shishido, A., & Ikeda, T. (2007). *Macromol. Rapid Commun.*, *28*, 1040.
[3] Häckel, M., Kador, L., Kropp, D., & Schimidt, H. W. (2007). *Adv. Mater.*, *19*, 227.
[4] Natansohn, A. & Rochon, P. (2002). *Chem. Rev.*, *102*, 4139.
[5] Andreozzi, L., Faetti, M., Galli, G., Giordano, M., & Palazzuoli, D. (2001). *Macromolecules*, *34*, 7325.

[6] Likodimos, V., Labardi, M., Pardi, L., Allegrini, M., Giordano, M., Arena, A., & Patanè, S. (2003). *Appl. Phys. Lett.*, *82*, 3313.
[7] Andreozzi, L., Bagnoli, M., Faetti, M., & Giordano, M. (2001). *Mol. Cryst. Liq. Cryst.*, *372*, 1.
[8] Angeloni, A. S., Caretti, D., Laus, M., Chiellini, E., & Galli G. (1991). *J. Polym. Sci., Polym. Chem. Ed.*, *29*, 1865.
[9] Andreozzi, L., Faetti, M., Giordano, M., Palazzuoli, D., Laus, M., & Galli, G. (2003). *Mol. Cryst. Liq. Cryst.*, *398*, 97.
[10] Ferry, J. D. (1980). *Viscoelastic Properties of Polymers*, Wiley: New York.
[11] Berghausen, J., Fuchs, J., & Richtering, W. (1997). *Macromolecules*, *30*, 7574.
[12] Colby, R. H., Gillmor, J. R., Galli, G., Laus, M., Ober, C. K., & Hall, E. (1993). *Liq. Cryst.*, *13*, 233.
[13] Andreozzi, L., Castelvetro, V., Faetti, M., Giordano, M., & Zulli, F. (2006). *Macromolecules*, *39*, 1880.
[14] Honerkamp, J. & Weese, J. (1993). *Rheol. Acta.*, *32*, 57.
[15] Andreozzi, L., Faetti, M., Giordano, M., Zulli, F., & Galli, G. (2005). *Mol. Cryst. Liq. Cryst.*, *429*, 383.
[16] Fetters, L. J., Lohse, D. J., Richter, D., Witten, T. A., & Zirkel, A. (1994). *Macromolecules*, *27*, 4639.
[17] Doi, M. & Edwards, S. F. (1986). *The Theory of Polymer Dynamics*, Oxford University Press: Oxford.